

1 A Small interfering RNA lead targeting RNA-dependent RNA-polymerase effectively
2 inhibit the SARS-CoV-2 infection in Golden Syrian hamster and Rhesus macaque

3

4 Se Hun Gu^{1,5}, Chi Ho Yu^{1,5}, Youngjo Song¹, Na Young Kim², Euni Sim², Jun Young Choi²,
 5 Dong Hyun Song¹, Gyeong Haeng Hur¹, Young Kee Shin^{2,3,4*} and Seong Tae Jeong^{1,*}

6

7 1 The 4th R&D Institute, Agency for Defense Development, Yuseong, P.O. Box 35, Daejeon
 8 34186, Republic of Korea

9 2 ABION Inc., R&D Center, Seoul 08394, Republic of Korea

10 3 College of Pharmacy and Research Institute of Pharmaceutical Sciences, Seoul National
 11 University, Seoul 08826, Republic of Korea

12 4 Molecular Medicine and Biopharmaceutical Sciences, Graduate School of Convergence
 13 and Technology, Seoul National University, Seoul, Republic of Korea

14 5 These authors contributed equally to this work.

15

16 * Correspondence should be addressed to S.T.J. (birdyjeong@add.re.kr) and Y.K.S.

17 (ykeeshin@snu.ac.kr)

18

19 **Abstract**

20

21 A small interfering RNA (siRNA) inhibitors have demonstrated the novel modality
 22 for suppressing infectious diseases. Sixty-one siRNA molecules, predicted by the
 23 bioinformatics programs, were screened for the possibility of treating severe acute respiratory
 24 syndrome coronavirus 2 (SARS-CoV-2) using an *in vitro* plaque assay. Among six siRNA
 25 leads with the efficacy of reducing plaque number, the siRNA targeting RNA-dependent
 26 RNA polymerase (RdRp) showed a reduction in SARS-CoV-2 infection-induced fever and
 27 virus titer in the Golden Syrian hamster and rhesus macaque. These results suggest the
 28 potential for RdRp targeting siRNA as a new treatment for the coronavirus disease 2019
 29 (COVID-19).

30

31 **Keywords:** SARS-CoV-2, Small interfering RNA, Syrian hamster, Rhesus macaque

32

33 **Introduction**

34

35 Coronaviruses (family *Coronaviridae*) are enveloped viruses with a positive-sense
 36 and single-stranded RNA genome. Some coronaviruses cause diseases of varying clinical
 37 severity, such as severe acute respiratory syndrome (SARS) and the Middle East respiratory
 38 syndrome (MERS) (1). More recently, SARS coronavirus 2 (SARS-CoV-2), which caused
 39 the coronavirus disease 2019 (COVID-19) pandemic, has infected approximately 11,301,850
 40 people and caused 531,806 deaths (as of July 6, 2020) globally (2). Despite the severity of the
 41 COVID-19 pandemic, there are no specific drugs except for a comprehensive treatment and
 42 management guide, which consist of symptomatic treatment, supportive therapy, and/or
 43 antiviral/antibiotic therapy. However, the comprehensive therapy shows different clinical
 44 outcomes for each patient because the efficacy and effectiveness of the therapy depends on
 45 the medical status of each patient. Current trials of repurposing of drugs for COVID-19 have
 46 shown no acceptable risk-benefit ratios except remdesivir and dexamethasone. However,
 47 there are several candidate drugs for COVID-19 treatment under research or clinical trials,
 48 such as antiretroviral drugs (HIV-1 protease inhibitor), RNA-dependent RNA polymerase
 49 (RdRp) inhibitors (remdesivir, favipiravir), antiviral cytokines (interferon β), and anti-spike
 50 protein monoclonal antibodies. Despite emergency use authorization of remdesivir for the
 51 treatment of severe COVID-19 patients, no drugs have been approved for COVID-19 so far.

52 RNA interference (RNAi) has a specific mechanism to silence gene expression by
 53 degrading messenger RNA (mRNA) targeted by small RNA molecules, such as microRNAs
 54 (miRNAs) and small interfering RNAs (siRNAs), which are complementary to mRNA (3, 4).
 55 Recently, it has been shown that RNAi specifically silences viral gene expression and treats
 56 infectious diseases caused by a viral infection (5, 6). Because RNAi treatments regulate gene
 57 expression inducing diseases, they have the advantage of being used to develop drugs against

infectious diseases that are difficult to treat using chemical or small-molecule compounds (6). Moreover, RNAi is an adequate method to deal with a pandemic because RNAi can be synthesized and tested in a very short time when the target sequence is identified.

Our goals in this study are to develop siRNAs to target and silence viral genes of SARS-CoV-2 for the inhibition of viral replication and treatment of COVID-19. In addition, since siRNAs can be used for versatile treatment against other types of coronavirus infections, the siRNAs were further selected by matching the target sequences in the highly conserved regions with SARS-CoV-1 or SARS-CoV-2 variants. It is expected to reduce the risk of ineffectiveness due to mutation at the target sequence (7). Among putative siRNA sequences targeting the conserved sequences of structure and replication genes, we obtained six siRNA leads that showed a reduction in cytopathic effect (CPE) and the plaque assay *in vitro*. Finally, we chose one of the most effective siRNAs that was less affected by mutation, and then performed *in vivo* experiments with siRNA in the Syrian hamster and rhesus macaque to confirm its protective efficacy against SARS-CoV-2.

This study indicates that siRNAs are a rapid and effective treatment for new emerging pathogens such as SARS-CoV-2, which may be able to diminish the impact of possible future pandemics by developing treatments promptly.

81 **Materials and Methods**

82

83 **Virus and cell culture**

84 SARS-CoV-2 isolated from a COVID-19 patient in Korea was used. The pathogen
85 resources (NCCP43326) for this study were provided by the National Culture Collection for
86 Pathogens (8). Viruses were propagated in Vero E6 cells (CRL 1586, American Type Culture
87 Collection, Manassas, VA, USA) and maintained in Dulbecco's modified Eagle's medium
88 (DMEM) supplemented with 2% heat-inactivated fetal bovine serum (FBS; GIBCO, USA), 2
89 mM L-glutamine, and antibiotics (penicillin/streptomycin) at 37°C for 3 days in a 5% CO₂
90 incubator. As determined using plaque assay, the infectivity titers of the SARS-CoV-2 stocks
91 were 2×10^6 plaque-forming units (PFU/mL).

92

93 **Design of siRNA targeting SARS-CoV-2**

94 In this study, we obtained the SARS-CoV-2 genome sequence of MT039890 from
95 (<https://www.ncbi.nlm.nih.gov/nuccore/MT039890>). We focused on seven regions of the
96 SARS-CoV-2 genome, namely the leader sequence, replicase polyprotein1a (pp1a), RdRp,
97 spike protein (S), nucleocapsid protein (N), membrane protein (M), and envelope protein (E)
98 to design specific siRNAs to inhibit viral replication. Potential siRNA sequences targeting
99 viral genes were predicted using the programs siDirect (<http://sidirect2.rnai.jp/>) and
100 VIRsiRNApred (<http://crdd.osdd.net/servers/virsimapred/>). Among the siRNAs predicted, we
101 examined whether siRNA predicted sequences that targeted the sequence of SARS-CoV, to
102 identify the 21 siRNA sequences targeting the conserved region in coronaviruses. We further
103 selected 40 siRNA sequences from the rest of the predicted siRNAs that did not match
104 SARS-CoV according to two criteria: first, siRNAs that have a score of less than off-target
105 effects in two portals; second, siRNAs that have low mutation rate among variants from

Nextstrain (<https://nextstrain.org/>). We finally obtained 61 putative siRNAs, all of which were 21-mer with dTdT at the 3'-overhang. The siRNAs were synthesized by Bioneer Co. (Daejeon, Republic of Korea).

***In vitro* efficacy test using Vero E6 cells (siRNA transfection)**

Vero E6 cells were inoculated into a 24-well plate, 1 mL each, through a 10% FBS DMEM without penicillin/streptomycin to ensure that the 24-well plate is 80–90% confluent. The next day, the Vero E6 cells were transfected with 100 nM siRNA using Lipofectamine RNAiMAX transfection reagent (Invitrogen, USA), according to the manufacturer's instructions. The cells were incubated at 37°C in 5% CO₂ for 3 h and washed with phosphate-buffered saline. Next, the SARS-CoV-2 stock of 1×10^5 PFU/mL was diluted at 1/100 into 1×10^3 PFU/mL. Next, 200 µL each was added to make the final 200 PFU. The Vero E6 cells were then infected with SARS-CoV-2 for 1 h 30 min. After infection, the supernatant was removed, changed with 2% FBS DMEM medium, and incubated at 37°C for 3 days in a 5% CO₂ incubator. The cells were observed daily for CPE using a microscope (Zeiss, Germany).

***In vitro* efficacy test using Vero E6 cells (plaque assay)**

To assess viral titers, a plaque assay was performed using Vero E6 cells in 6-well culture plates. Briefly, subconfluent monolayers of Vero E6 cells were inoculated with 10-fold serial diluents and incubated at 37°C for 1 h 30 min in a 5% CO₂ incubator. After incubation, the supernatant was removed and carefully overlaid with 1 mL/well of overlay solution (1:2 mixtures of 1% agarose and 2% FBS DMEM) and incubated for 3 days. The plates were then fixed and inactivated using a 4% formaldehyde solution and stained with 0.1% crystal violet.

RNA extraction and cDNA synthesis. Total RNA was extracted from supernatants and animal tissues using the PureLink RNA mini kit (Invitrogen, San Diego, CA, USA) according to the manufacturer's instructions. cDNA was synthesized using the SuperScript III First-Strand Synthesis Systems (Invitrogen) and then analyzed for SARS-CoV-2 RNA using qRT-PCR.

***In vitro* efficacy test using Vero E6 cells**

The primers and probe targeting the SARS-CoV-2 E gene and the forward and reverse primer sequences for real-time PCR were 5'-ACAGGTACGTTAATAGTTAATAGCGT-3' and 5'-ATATTGCAGCAGTACGCACACA-3', respectively, and the probe was 5'-ACACTAGCCATCCTTACTGCGCTTCG-3' (9). The probe was labeled with the reporter dye 6-carboxyfluorescein at the 5'-end and quencher dye Black Hole Quencher 1 at the 3'-end, respectively. Each 20-μL reaction mixture contained 2 μL cDNA, 10 μL 2X TaqMan Gene Expression master mix (Applied Biosystems, USA), 0.5 μL forward and reverse primers (36 μM), 0.5 μL fluorescent probe (10 μM), and 6.5 μL double deionized water. The reaction was performed at 50°C for 2 min and 90°C for 10 min, followed by 40 cycles at 95°C for 15 s and 60°C for 1 min, in a QuantStudio 6 Flex Real-Time PCR system (Applied Biosystems, USA). The standard curve was constructed using RNA from SARS-CoV-2 infected Vero E6 cells. RNA concentration was measured using a NanoDrop spectrophotometer. After RT-PCR using random primers (10 μM), 10-fold serial dilutions of the cDNA were used in duplicate to generate a standard curve.

Animal experiments.

We assessed the therapeutic efficacy of siRNA in the Syrian hamster and rhesus macaque and established a model for SARS-CoV-2 infection (10, 11). First, we confirmed

whether Syrian hamsters were infected with SARS-CoV-2; 6-week-old male Syrian hamsters were randomly segregated into 5 groups. Each group of the animals was inoculated with 40,000 PFU of SARS-CoV-2 via the intranasal route. At 2 days post-infection (d.p.i.), the lungs were harvested for qRT-PCR analysis. Next, we evaluated the therapeutic efficacy of siRNA in the Syrian hamsters. SARS-CoV-2 inoculation of the animals was performed through intranasal instillation of 1,000 PFU per head. Four hours after virus inoculation, the animals in groups 2 and 3 were intranasally administered with siRNA (No. 14) 17.3 µg (low dose) and 34.6 µg (high dose), respectively (Table 2). At 2 d.p.i., the lungs were harvested for further analysis.

Third, we assessed the therapeutic efficacy in the rhesus macaque. Three male rhesus macaques were randomly segregated into three groups of one each (Table 3). The animals were inoculated with 4.0×10^6 PFU of SARS-CoV-2 through intranasal and intratracheal routes under anesthesia. After 4 and 24 h, the animals in groups 2 and 3 were intratracheally administered with siRNA (No.14) 2 mg/kg (low dose) and 4 mg/kg (high dose), respectively, under anesthesia. All the animals were monitored daily for clinical signs, body weight, and body temperature. Swab samples, including nasal, oropharyngeal, and rectal swabs, were collected. The animals were euthanized at 3 d.p.i. All inoculations and handling of the animals, as well as the method of euthanasia and collection of tissues, were performed according to well-established protocols approved by the Institutional Animal Care and Use Committee of the Agency for Defense Development (ADD-IACUC-20-12 and ADD-IACUC-20-13). All experiments were conducted in consultation with the veterinary and animal care staff of the ADD animal biosafety level-3 (ABSL-3) containment, in a facility in which other respiratory disease-causing coronaviruses had never been handled.

Results

Design of siRNA targeting SARS-CoV-2

To design a siRNA targeting SARS-CoV-2, siRNA molecules were screened from the whole sequence of SARS-CoV-2 (SNU-MT039890). We designed siRNA sequences and then selected a siRNA that targeted the conserved sequence of SARS-CoV-2 for application in the treatment of various strains of SARS-CoV-2. To target the S proteins, we designed siRNAs in the less mutated region (HR2) and receptor binding motif (RBM). Among sixty one siRNA sequences expected to inhibit SARS-CoV-2 infection, twenty one siRNAs, targeting leader sequence, RdRp, S, and N, were primarily selected as the conserved region sequences of coronavirus. Additionally, forty siRNA sequences, targeting pp1a, RdRp, S, N, E, and M, were designed to be most conserved for SARS-CoV-2 and its mutants. All siRNA candidates were 21-mer by adding two deoxythymidine (dTdT) at the 3' overhang to enhance siRNA stability and binding efficiency to target RNA (12).

Selection of efficient siRNA leads using *in vitro* efficacy test

We tested the efficacy of siRNAs to inhibit viral infection in the Vero E6 cells, in which the CPE can be confirmed by apoptosis upon SARS-CoV-2 infection and plaque reduction assay (13). After the Vero E6 cells were infected with 200 PFU of SARS-CoV-2 and treated with 100 nM of the 61 siRNA sequences, the CPE and plaque assays were performed at 3 d.p.i. (Fig. 1a-1c). At 3 d.p.i., all siRNA candidates reduced CPE in SARS-CoV-2 infected Vero E6 cells, while CPE was observed in the control group (data not shown). Based on the results of the CPE and plaque assays, we selected six siRNA leads, showing a reduction in plaque number. Six siRNA leads were subjected to the NCBI blast to ensure that they did not target any human genes. RdRp, pp1a, and N mRNAs were targeted by 3 siRNAs (Nos. 9, 14, and 36), 2 siRNAs (No. 26 and 29), and 1 siRNA (No. 61), respectively.

The Nextstrain website was used to monitor the data on SARS-CoV-2 mutation and to confirm whether the regions targeted by our siRNA leads were less mutated (as of June 26, 2020). Mutation rates in siRNA-targeted regions were 0-0.002%, indicating that siRNA leads can be used to treat most SARS-CoV-2 strains. Hence, the six siRNA leads were effective in reducing viral replication *in vitro* and less influenced by SARS-CoV-2 mutation (Table 1).

Efficacy test of the No. 14 siRNA lead against SARS-CoV-2

With six siRNAs, we examined whether the replication of SARS-CoV-2 was inhibited using a plaque reduction assay. Vero E6 cells were infected with 500 PFU of SARS-CoV-2 with or without siRNA candidates and the plaque assay was performed at 3 d.p.i. From the results, lead siRNA No. 14 (out of the six candidates) showed the least plaque formation (data not shown). To calculate the half-maximal effective concentration (EC_{50}), the Vero E6 cells infected with 500 PFU of SARS-CoV-2 were treated with the siRNA No. 14 in a dose-dependent manner (5-100 nM) (Fig. 2a-2i). Then, the CPE assay was performed at different time points. The CPE started to reduce with 20 nM of the siRNA No. 14, and cell morphology was similar in cells treated with 100 nM of the siRNA No. 14. EC_{50} was further calculated using qRT-PCR to determine the copy number of SARS-CoV-2 (Fig. 2m). From the result, EC_{50} of the siRNA No. 14 was approximately 9.7 nM at 2 d.p.i. in 500 PFU SARS-CoV-2 infected Vero E6 cells. Recently, it was reported that EC_{50} of the antiviral drugs, remdesivir, chloroquine and nafamostat, known to be effective for COVID-19 (14).

Clinical signs in golden Syrian hamsters and rhesus macaques

To assess the therapeutic efficacy of siRNA in the hamsters, three groups were formed composed of a control group and two treatment groups (Table 2). At 2 d.p.i., the control hamsters showed a hunched posture, ruffled hair, and mild cough. However, clinical signs such as cough were not observed in the siRNA No. 14-treated hamsters. The three rhesus macaques consisted of one control animal and two treatment animals (Table 3). After anesthetizing the animals, three male rhesus macaques were inoculated with 4×10^6 PFU SARS-CoV-2, administered at a dose of 5 mL through intratracheal (4 mL) and intranasal (1 mL) instillation. After 4 and 24 h, we administered the siRNA No. 14 through the same route at low (2 mg/kg; G2) and high (4 mg/kg; G3) doses, respectively. At 1 d.p.i., diarrhea was observed in the viral control and body temperature was markedly elevated compared to the base level (Fig. 3c). SARS-CoV-2-infected rhesus macaques (G1) had elevated body temperature, from 38.6-40.4°C, between 1 and 2 d.p.i. Interestingly, high-dose siRNA No. 14-treated animals (G3) showed a base level of body temperature over 3 days. All treated animals displayed normal appetite and behavior.

qRT-PCR analysis of the Syrian hamsters and rhesus macaques

To confirm infection of SARS-CoV-2 in the hamster, we inoculated each group with 4-40,000 PFU SARS-CoV-2 by the intranasal route. SARS-CoV-2 RNA was detected in all hamsters, including the 4 PFU inoculation group (data not shown). We assessed the therapeutic efficacy of the siRNA No. 14 in the hamsters and analyzed the lung of the hamsters at 2 d.p.i. using qRT-PCR. The results showed that the number of viral RNA copies from the lung tissue of the siRNA No. 14-treated hamsters markedly decreased by approximately 10^4 viral copies compared to that of the control hamsters (Fig. 3a). Next, we

251 investigated viral copies from the trachea of rhesus macaques at 3 d.p.i. using qRT-PCR. The
252 number of viral RNA copies in the siRNA No. 14-treated rhesus macaques significantly
253 decreased by approximately 10^3 viral copies compared to that in the control animals (Fig. 3b).
254 These results indicate that siRNA No. 14 effectively inhibited SARS-CoV-2 infection and
255 replication in the lung and upper respiratory tract.

256

Discussion

An effective SARS-CoV-2 treatment is needed to end the COVID-19 pandemic in the near future. To date, many reports have demonstrated that RNAi is a powerful method for gene silencing, including virus infection and replication *in vitro*, *in silico* and *in vivo* (15, 16, 19) against SARS-CoV. Wang et al presented that SARS-CoV replication was efficiently inhibited by siRNA in Vero cells. Li et al demonstrated that siRNA was significantly effective in prophylactic and therapeutic regimen against SARS-CoV in Rhesus macaques (19). More recently, a CRISPR/Cas13d system was reported for the therapeutic agent of SARS-CoV-2 (20). In addition, Chen et al showed theoretical predictions of the potential siRNA targets by computation modeling in the SARS-CoV-2.

Animal studies on SARS-CoV-2 play an important role in understanding the pathogenesis and development of therapeutic drugs. Recently, animal studies on SARS-CoV-2 have reported that rhesus monkeys and transgenic mice expressing human ACE2 receptor were susceptible to SARS-CoV-2 infection (17, 18). In addition, the pathogenesis and transmission of SARS-CoV-2 were shown in Syrian hamsters (10). Efficacy test using siRNA therapeutics for SARS-CoV-2 has been reported not yet in the hamster and rhesus macaque. However, efficacy tests including DNA vaccines and therapeutic antibody were reported in the SARS-CoV-2 animal models (21, 22). The Syrian hamster model was used for demonstrating protective efficacy of neutralizing antibodies against SARS-CoV-2. The hamsters showed typical clinical signs within one week after virus inoculation. Rhesus macaque model was used for DNA vaccine test. Rhesus monkeys developed humoral and cellular immune responses and, were protected against SARS-CoV-2.

In this study, to demonstrate the siRNAs that are effective for the inhibition of

281 SARS-CoV-2 infection, we tested 61 siRNA duplexes in Vero E6 cells. Among them, the best
 282 lead, siRNA No. 14, showed strong inhibitory efficacy against SARS-CoV-2 infection and
 283 replication in Vero E6 cells. To assess the inhibition efficacy of siRNA No. 14 for SARS-
 284 CoV-2 in animals, we used Syrian hamsters and rhesus macaques. Our data showed that
 285 SARS-CoV-2 viral RNA decreased in the siRNA No. 14-treated animals. Additional research
 286 is warranted to determine the possibility of siRNA treatment for COVID-19. Further studies
 287 would also be needed to address the safety and effective delivery methods of siRNA.
 288

289 **Acknowledgements**

290 This work was supported by grants (011555-912664201) from the Agency for

291 Defense Development, Republic of Korea.

292

References

1. Wu, A., et al. Genome composition and divergence of the novel coronavirus (2019-nCoV) originating in China. *Cell Host Microbe*. (2020).
2. WHO Coronavirus Disease (COVID-19) Dashboard, <http://covid19.who.int>.
3. Bernstein, E., et al. Role for a bidentate ribonuclease in the initiation step of RNA interference. *Nature*. (2001).
4. McManus, MT., et al. Gene silencing in mammals by small interfering RNAs. *Nature reviews genetics*. (2002).
5. Fischer, LT., et al. a new therapeutic strategy against viral infection. *Cell research*. (2004).
6. Lopez-Fraga, M., et al. RNA interference-based therapeutics: new strategies to fight infectious disease. *Infectious Disorders-Drug Targets. Formerly Current Drug Targets-Infectious Disorders*. (2008).
7. Boden, D., et al. Human immunodeficiency virus type 1 escape from RNA interference. *Journal of Virology*. (2003).
8. Kim, JM., et al. Identification of coronavirus isolated from a patient in Korea with COVID-19. *Osong Public Health and Research Perspectives*. (2020).
9. Corman, VM., et al. Detection of 2019 novel coronavirus (2019-nCoV) by real-time RT-PCR. *Euro Surveill*. (2020).
10. Sia, SF., et al. Pathogenesis and transmission of SARS-CoV-2 in golden hamsters. *Nature*. (2020).
11. Munster, VJ., et al. Respiratory disease in rhesus macaques inoculated with SARS-CoV2. *Nature*. (2020).
12. Elbashir, SM., et al. Functional anatomy of siRNAs for mediating efficient RNAi in *Drosophila melanogaster* embryo lysate. *The EMBO journal*. (2001).

13. Severson, WE., et al. Development and validation of a high-throughput screen for inhibitors of SARS CoV and its application in screening of a 100,000-compound library. *Journal of biomolecular screening*. (2007).
14. Wang, M., et al. Remdesivir and chloroquine effectively inhibit the recently emerged novel coronavirus (2019-nCoV) in vitro. *Cell research*. (2020).
15. Wang, Z., et al. Inhibition of Severe Acute Respiratory Syndrome Virus Replication by Small Interfering RNAs in Mammalian Cells. *Journal of Virology*. (2004).
16. Chen, W., et al. Computational identification of small interfering RNA targets in SARS-CoV-2. *Virologica Sinica*. (2020).
17. Shan, C., et al. Infection with Novel Coronavirus (SARS-CoV-2) causes pneumonia in the Rhesus macaques. *Research square*. (2020).
18. Bao, L., et al. The pathogenicity of SARS-CoV-2 in hACE2 transgenic mice. *BioRxiv*. (2020).
19. Li et al. Using siRNA in prophylactic and therapeutic regimens against SARS coronavirus in Rhesus macaque. *Nature* (2005).
20. Nguyen et al. Virus against virus: a potential treatment for 2019-nCoV(SARS-CoV-2) and other RNA viruses. *Cell Research* (2020)
21. Rogers et al. Isolation of potent SARS-CoV-2 neutralizing antibodies and protection from disease in a small animal model. *Science* (2020).
22. Yu et al. DNA vaccine protection against SARS-CoV-2 in rhesus macaques. *Science* (2020).

340 **Author Contributions**

341 S.H.G., C.H.Y. Y.K.S. and S.T.J. conceived and designed the experiments; S.H.G.,
342 C.H.Y. and Y.S. performed the experiments; S.H.G., C.H.Y., Y.S., N.Y.K., E.S., J.Y.C.,
343 D.H.S., G.H.H., Y.K.S. and S.T.J. analyzed the data and prepared the figures; and all authors
344 prepared and reviewed the manuscript.

345

346 **Competing interests**

347 The authors have no conflicts of interest.

348

349 **Table 1.** The sequences of siRNA targeting SARS-CoV-2.

No.	siRNA	Target gene (position)	Target sequence (5'-3') Guide RNA (5'-3')	Mutation site (2020-06-26)	Mutation cases
9	N14-R2	RdRp (1,206-1,228)	CAAUGUUGCUUUUCAAACU AGUUUGAAAAGCAACAUUGdTdT	CAAUGUUGCUUUUCAAACU :A → C, 1 case CAAUGUUGCUUUUCAAACU :G → A, 5 cases CAAUGUUGCUUUUCAAACU :C → T, 1 case	7 cases (0.002%)
14	N14-R7	RdRp (2,622-2,644)	GGAGUAUGCUGAUGUCUUU AAAGACAUCAGCAUACUCCdTdT	GGAGUAUGCUGAUGUCUUU :G → T, 1 case GGAGUAUGCUGAUGUCUUU :A → C, 1 case GGAGUAUGCUGAUGUCUUU :G → A, 1 case	3 cases (0.001%)
26	N26-El_105	pp1a (1,135-1,153)	GGACCUGAGCAUAGUCUUG CAAGACUAUGCUCAGGUCCdTdT	GGACCUGAGCAUAGUCUUG :G → A, 3 cases GGACCUGAGCAUAGUCUUG :C → T, 2 cases GGACCUGAGCAUAGUCUUG :C → T, 2 cases	7 cases (0.002%)
29	N29-El_108	pp1a (5,652-5,670)	GGAUGGUGUUGUUUGUACA UGUACAAACAACACCAUCCdTdT	-	0 case (0.000%)
36	N36- El_1015	RdRp (2,518-2,536)	CCGGCUGUUUUGUAGAUGA UCAUCUACAAAACAGCCGGdTdT	CCGGCUGUUUUGUAGAUGA :C → T, 3 cases CCGGCUGUUUUGUAGAUGA :A → G, 3 cases	6 case (0.002%)
61	N61- El_908	N (931-949)	GCUUCAGCGUUCUUCGGAA UUCCGAAGAACGCUGAAGCdTdT	GCUUCAGCGUUCUUCGGAA : C → T, 1 case GCUUCAGCGUUCUUCGGAA : G → T, 1 case GCUUCAGCGUUCUUCGGAA :C → T, 2 cases	4 cases (0.001%)

350

Table 2. Study design of Syrian Hamsters.

Group	Sex	Age (weeks)	No. of Animals	Virus inoculation	siRNA Dose	Dose regimen
G1	Male	6	5	§IN, 1.0x10 ³ PFU/head	0	-
G2	Male	6	5	§IN, 1.0x10 ³ PFU/head	17.3ug/head	+4h
G3	Male	6	5	§IN, 1.0x10 ³ PFU/head	34.6ug/head	+4h

§ IN, Intra Nasal

Table 3. Study design of rhesus macaques.

Group	Sex	Age (years)	Body weight (kg)	Virus inoculation	siRNA Dose	Dose regimen	Total dosage
G1	Male	5	5.4	¶IN, IT, 4.0x10 ⁶ PFU/head	0	-	-
G2	Male	4	3.5	¶IN, IT, 4.0x10 ⁶ PFU/head	2mg/kg	+4h, +24h	14mg
G3	Male	4	3.0	¶IN, IT, 4.0x10 ⁶ PFU/head	4mg/kg	+4h, +24h	24mg

¶ IN, Intra Nasal. IT, Intra Trachea

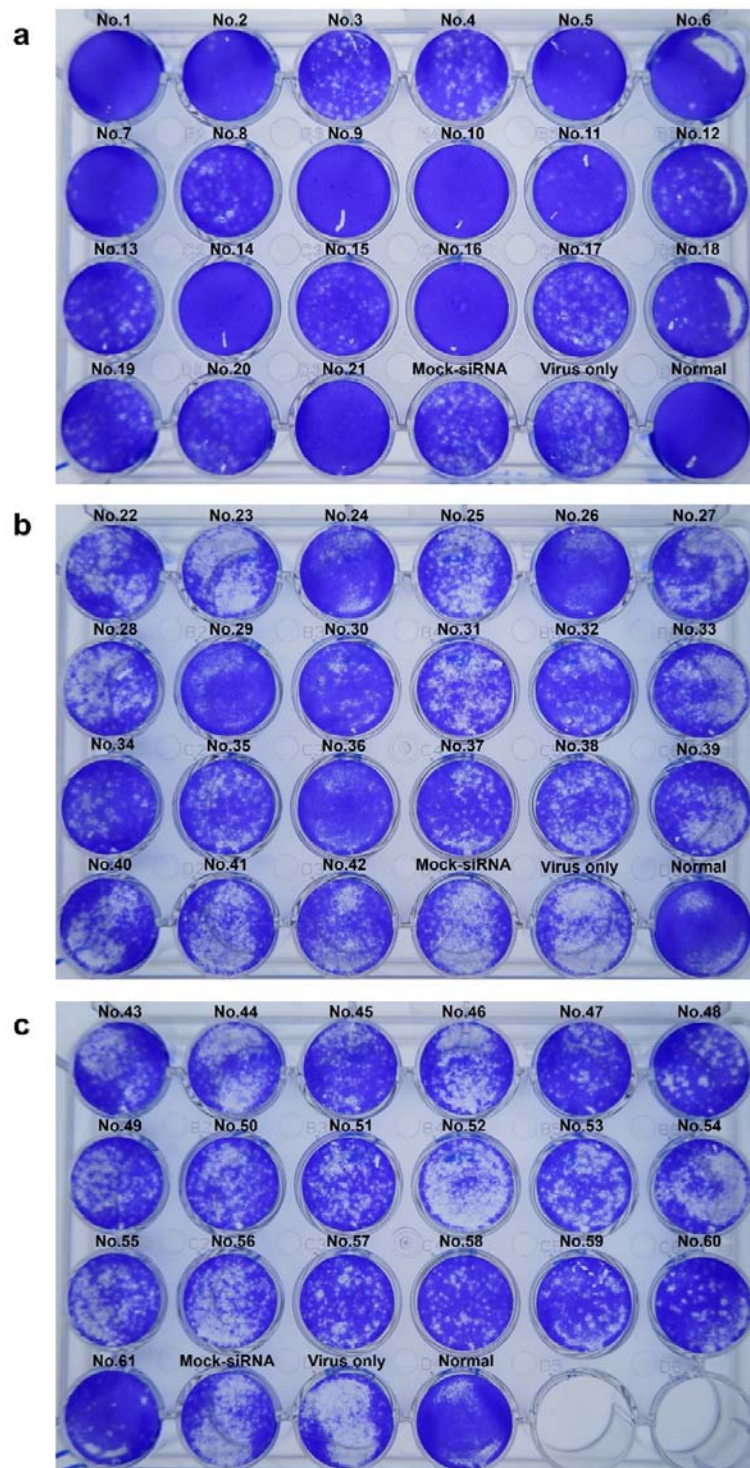
Figure Legends

Fig. 1. Screening of siRNA molecules for SARS-CoV-2 using plaque assay. (a) siRNA No. 1-21. (b) siRNA No. 22-42. (c) siRNA No. 43-61.

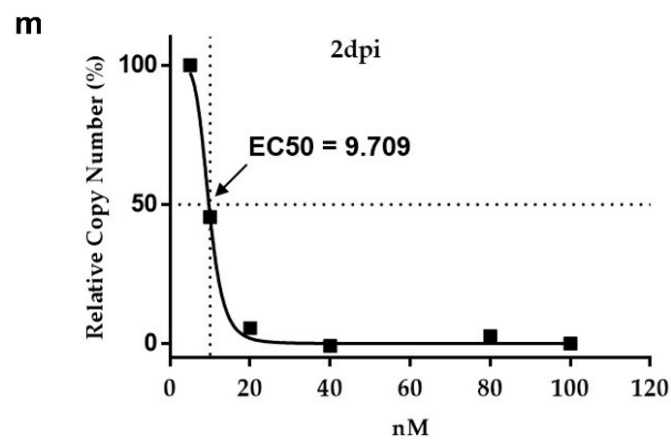
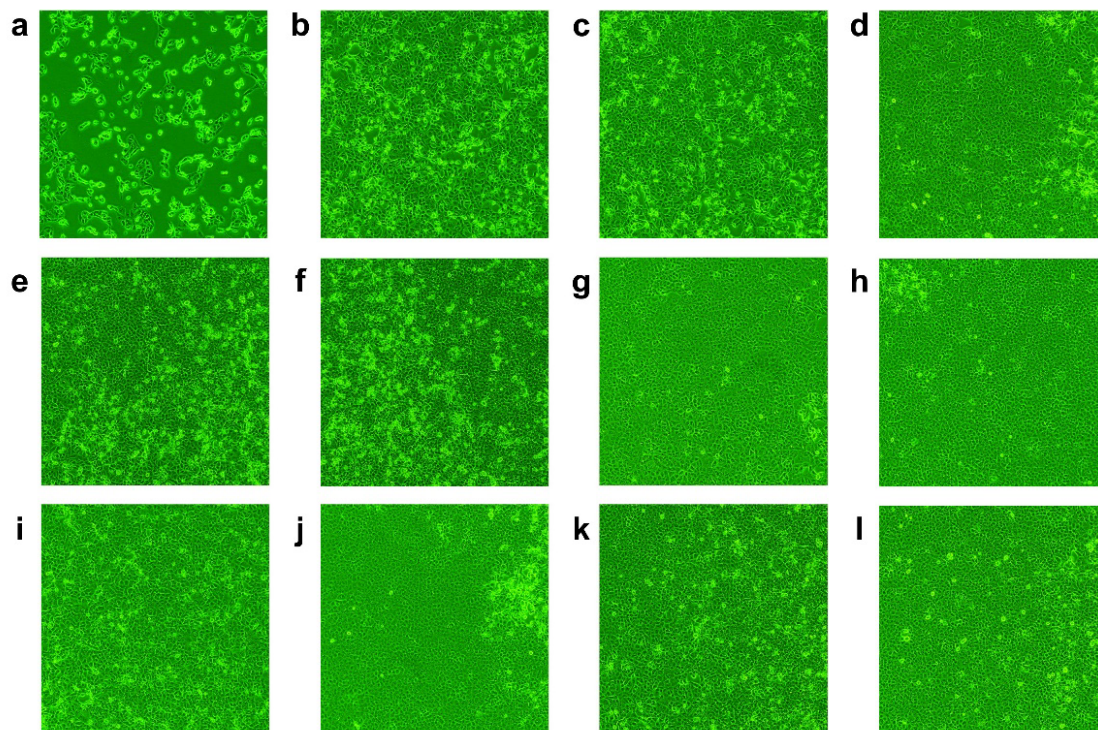
Fig. 2. siRNA No. 14 inhibition of SARS-CoV-2 cytopathicity in Vero E6 cells (CPE assay and EC₅₀). Vero E6 cells were infected with SARS-CoV-2 and incubated for 2 days. (a) Mock-siRNA (100 nM). (b) 5 nM. (c) 10 nM. (d) 20 nM. (e) 30 nM. (f) 40 nM. (g) 50 nM. (h) 60 nM. (i) 70 nM. (j) 80 nM. (k) 90 nM. (l) 100 nM. (m) EC₅₀ of siRNA No. 14 using qRT-PCR.

Fig. 3. qRT-PCR of viral RNA copies in lung of Syrian hamsters and trachea of rhesus macaques inoculated with SARS-CoV-2, respectively. Viral RNA copies per 1 µg of total RNA are sacrificed on 2 and 3 d.p.i. (a) Syrian hamsters. (b) Rhesus macaques. (c) Body temperature change of rhesus macaques.

Fig. 1.



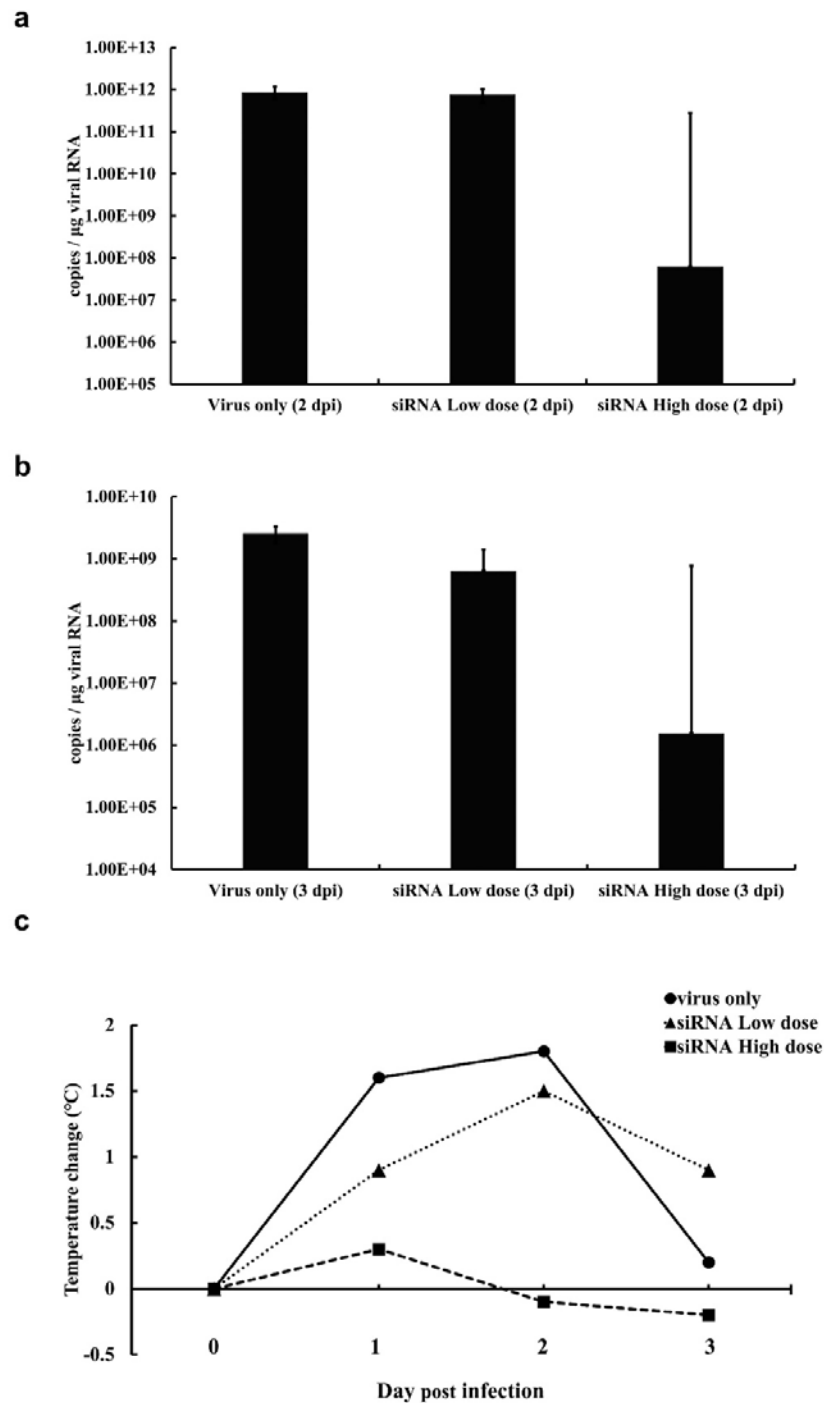
380 **Fig. 2.**



381

382

383 **Fig. 3.**



384

385